EFFECTS OF ADVERSE WIND ON THE PHASE VELOCITY OF MECHANICALLY GENERATED WATER WAVES

MIZUNO, Shinjiro
Research Institute for Applied Mechanics, Kyushu University : Associate Professor

MITSUYASU, Hisashi
Research Institute for Applied Mechanics, Kyushu University : Professor

https://doi.org/10.5109/7172639

出版情報：Reports of Research Institute for Applied Mechanics. 21 (68), pp.33-52, 1973. 九州大学応用力学研究所

Reports of Research Institute for Applied Mechanics
Vol. XXI, No. 68, 1973

EFFECTS OF ADVERSE WIND ON THE PHASE VELOCITY OF MECHANICALLY GENERATED WATER WAVES

By Shinjiro Mizuno* and Hisashi Mitsuyasu**

Mechanically generated waves propagating against an adverse wind are measured at six stations along the test section of a wind-wave tunnel for wave periods, T = 0.8, 1.0 and 1.2 sec and for wind speed range from 2.5 to 12.5 m/sec. All wave data are converted to digital form and a harmonic analysis of the data is made using a FFT procedure. The phase speed of the waves is determined from the phase difference between the fundamental frequency compoments of the wave data at any two stations.

The theoretical study is made on the effects of an adverse wind on the wave speed. The first order solutions of wave speed are obtained by solving the invicid Orr-Sommerfeld equation for the air and the water flow respectively, and both are combined with each other by the dynamical condition at the water surface. It is assumed that the wind profile consists of a logarithmic distribution and a uniform free stream distribution, and that the drift current profile consists of a parabolic distribution and no current part. The theoretical solutions for the wave speed agree very well with the experimental results.

1. Introduction

The wind blowing over the water waves produces a marked change of wave speed as well as new generation of overlapping wind waves. The drift current caused by wind shear stress or Stoke's mass transport due to wind-generated waves is the primary factor which changes the phase speed of water waves. Under an assumption that the surface drift current is much less than the wave speed, Lilly[1] developed a perturbation method for obtaining wave speed solutions when the current velocity profile was given as a function of depth, and particularly applied it to the case of a laminar parabolic flow profile with zero net transport. Kato[2] calculated the wave speed solutions to the second order using a somewhat different parabolic current profile, and obtained somewhat unexpected results that the second order solutions are negligible even when the ratio of surface drift current to wave speed is relatively large.

* Associate Professor, Research Institute for Applied Mechanics, Kyushu University, Fukuoka, Japan.

** Professor, Research Institute for Applied Mechanics, Kyushu University, Fukuoka, Japan.

According to Miles' expression, wave speed is also influenced by the in-phase component to the surface displacement of wave-induced pressure fluctuations at the water surface. Therefore, it will be necessary to make the wave speed corrections not only for the water flow but also for the air flow in such a case that both contributions to the wave speed are nearly of the same order of magnitude. Shemdin[3] was the first to obtain the wave speed solutions with consideration for both the effects.

In this paper we firstly describe the experimental results of wave speed measurements in the case that mechanically generated waves travel in the direction opposite to the wind. Secondly, starting from the invicid Orr-Sommerfeld equation, we obtain the first order solution for the wave-speed correction due to the air and water flow respectively. Then, the wave speed is given in the following form

$$\frac{C}{C_0}=1+\frac{C_a}{C_0}+\frac{C_w}{C_0}\ ,$$

where C/C_0 is the wave speed solution nondimensionalyzed with respect to the phase speed of a free wave C_0, C_w/C_0 and C_a/C_0 being the first order solutions of the wave speed corrections due to the water and air flow respectively. Finally, the theoretical solution is compared with the experimental results.

2. Experiments

2.1. Experimental Apparatus and Procedures

Experiments were made in a wind-wave tunnel 0.6 m wide by 0.8 m high whose glass test section has a length of 13.4 m. Water depth was kept 0.35 m throughout the experiment. A centrifugal fan controled the air discharge through the tunnel. The wind was made uniform by honeycombs and a number of fine mesh screens at the inlet section and discharged from air duct just upstream of a wave generator, as shown in Fig. 1. To thicken the boundary layer, roughened transition plates were installed at the inlet and outlet* of the test section, so that the effective length of measurements, i.e., the maximum fetch, was about 8.5 m downstream of the end of the upwind transition plate. A sloping beach of wooden plate covered with scrubbing-brushes was installed at the inlet side of the wave tank to prevent reflection of waves which were generated by the wave generator at the opposite end. Furthermore, wave filters of wire gauzes were installed ahead of the sloping beach, and also ahead of the wave generator to prevent reflection of wind waves from the plate of the wave generator.

Measurements of waves were made simultaneously at six locations with resistance-type wave gages each of which uses a double 1.0 mm diameter platinum wire. The stations of the wave gages were arranged from the location

* The transition plate at the outlet is not necessary needed for the present experiment but equipped for the experiment of a favorable wind in near future.

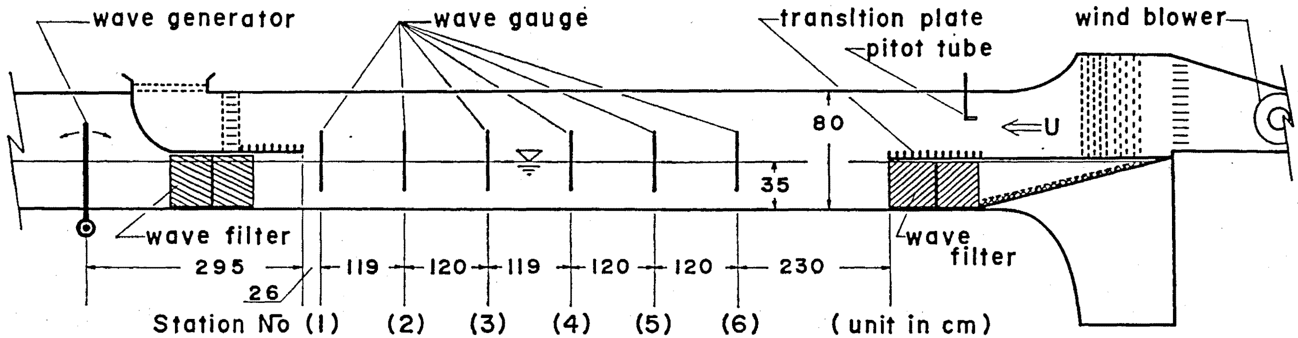

Fig. 1 Sketch of experimental apparatus.

of 26 cm ahead of the tip of the downwind transition plate in the order of 1, 2, 3, 4, 5, 6 at a distance of about 1.2 m along the test section. Vertical wind velocity profiles were measured at the center of three stations (No. 2, 4, 6) using a standard Pitot tube, and a reference air velocity U_r was defined as the free stream velocity over the upstream transition plate.

The wave generator operated about 2 minutes after the wind had begun to blow. Mechanically generated waves propagated through the test section against the wind waves and at the same time all signals of six wave gages were recorded on a magnetic tape for five minutes.

For analysis of the wave data, 32 waves, which were taken from the wave record 2 minutes after the start of the wave generators, were fed into an 8 channel A-D converter. The sampling rate of the converter was selected to be 64 data points per wave. In order to avoid "leakage" error in the discrete Fourier transform it would be important to take the data length T_n to be exactly 32 times wave period. For this purpose the sampling intervals were adjusted slightly at every wave datum to reduce below 5 % the errors of wave amplitudes of mechanically generated waves at the fundamental frequency. The A-D converter transmitted the digital signals to the digital tape recorder. The digital tape were processed on a FACOM 270-20 computer. The discrete Fourier transform of each record was calculated using the 'fast Fourier transform' algorithm. The complex Fourier coefficients at the fundamental frequency of the waves were used for calculating the amplitude and phase of waves.

2.2. Experimental Resnlts

Air velocity profiles over the water surface were measured for both cases of wind waves alone and of the coexistence system of wind waves and mechanically generated waves of period 1.0 sec and height 2 cm. Fig. 2 shows a typical example of a semilogarithmic plot of the air velocity profiles measured for both the cases for air speed in the range from 5 m/sec to 15 m/sec. We can see that the experimental data fit straight lines quite well, thus confirming that the air velocity profile is logarithmic with height from a few centimeters above the water surface to a height of 30 cm at the station 2. Values of U_* and Z_0 were calculated by applying each set of the wind data to the logarithmic law, where U_* is the friction velocity of the air and Z_0 the roughness parameter. All of the results are summarized in Table 1.

Experimental values of U_* increased only slightly by the presence of mechanically generated waves except at the station 2. This is perhaps because the wind shear layer separated from the upwind transition plate reattached to the water surface earlier near the crest of mechanically generated waves and caused the generation of weve ripples earlier than in the case of the absence of mechanically generated waves.

The amplitude and phase of waves were obtained from the complex Fourier coefficients of the fundamental frequency of mechanically generated waves each

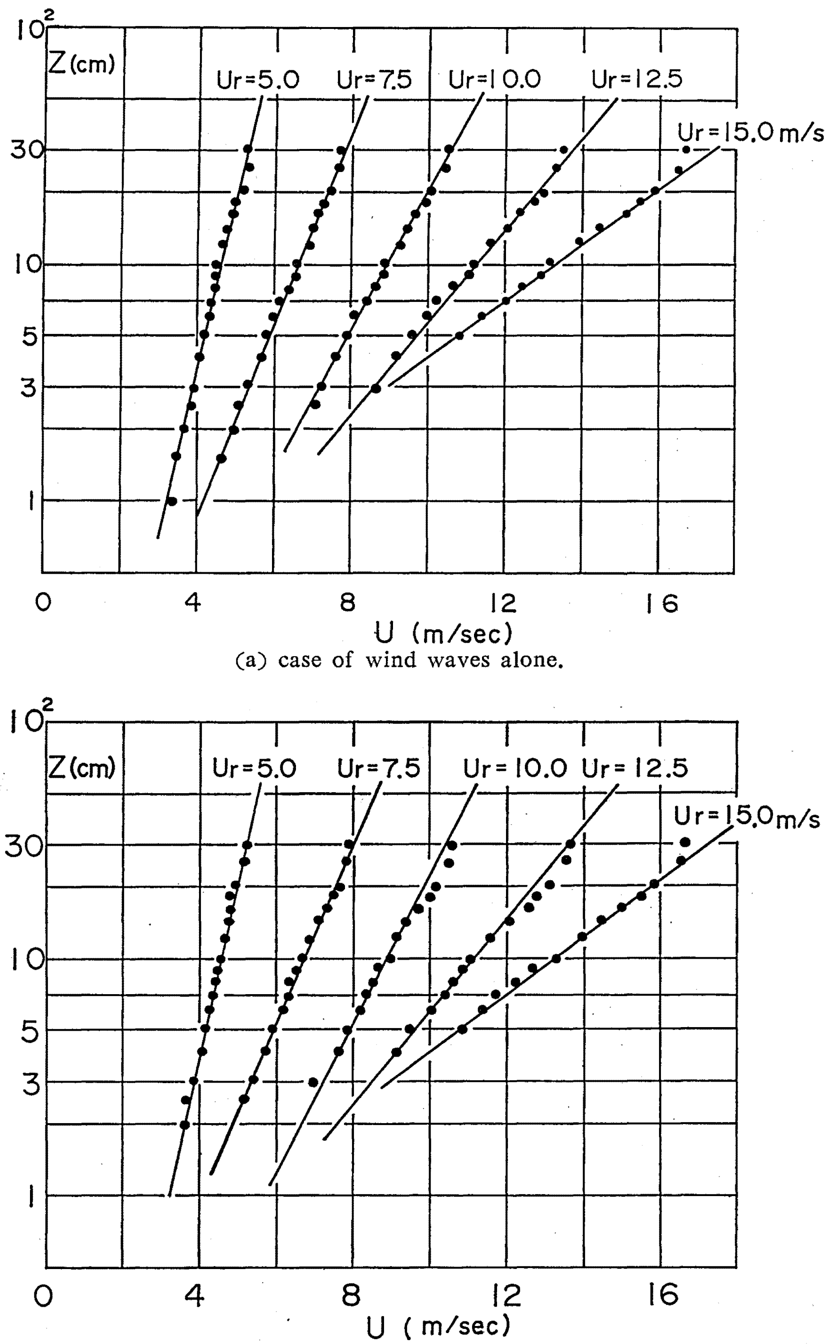

(a) case of wind waves alone.

(b) case of coexistence system of wind waves and mechanically generated waves.

Fig. 2 Semilogarithmic wind speed profiles plotted for various wind velocities at Staion 2.

at six stations. The wave length was obtained from the distance and the phase difference plus number of waves contained between any two stations, and from the wave length and period the phase speed was calculated. The phase speed was obtained for waves of periods in the range 0.8–1.2 sec., wave height in the range 1.5–4.0 cm, and the reference air velocity U_r from 0 to 12.5 m/sec. The results are summarized in Table 2, and also shown in Fig. 3 as a function of U_r by taking wave period as a parameter, where both C and U_r are normalized by C_0, that is, by the zeroth order phase speed of mechanically generated wave at still water.

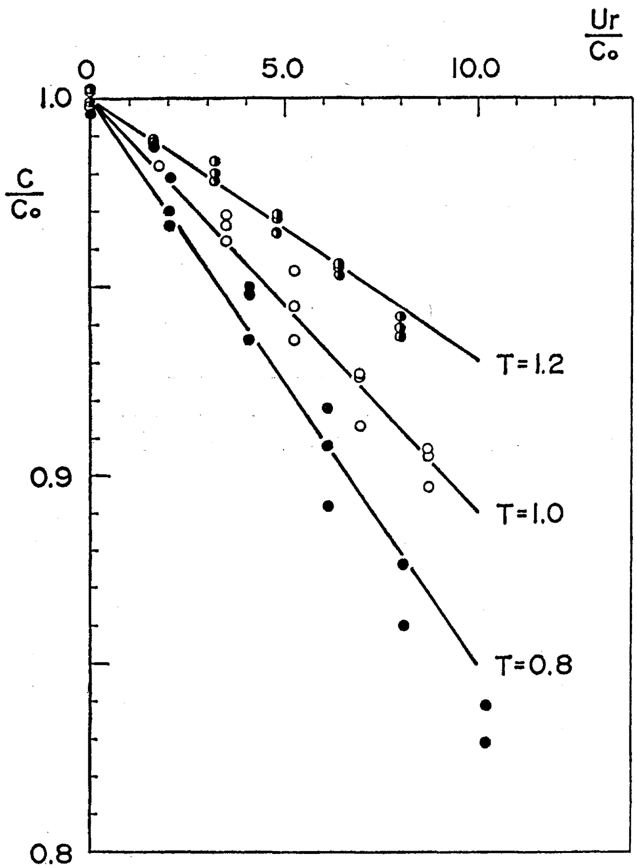

Fig. 3 Dependence of phase speed on wind speed.

It can be seen that the phase speed decreases with an increase of the reference air velocity U_r and does not much vary with the propagation of waves, and that although the relationship between C and U_r is approximately linear, the phase speed has a tendency to increase more rapidly at high wind velocity than at low velocity.

Shemdin made similar measurements when the wind and waves were in the same direction. In a favorable wind the phase speed increased with wind speed. Fig. 4 shows the comparision of phase speed as a function of U_r for waves of different frequencies in both a favorable and an adverse wind condition. Although we should refrain from making a precise comparison because the experimental conditions are different between Shemdin and us, it should be noted that for waves of the same period, the rate of decrease of phase speed with wind speed in an adverse wind condition is distinctly greater than that of increase in a favorable condition.

Although we attempted to make measurements of drift current profiles by using small paper discs as floats, most discs hardly drifted horizontally in the wind-stirred surface layer after they were released and the attempt resulted in a failure, so that we made measurements of the surface drift current U_w alone and the current profiles were observed by a flow visualization tequnique.

The surface current was obtained by measuring with a stop watch the time interval during which the floats of 6 mm in diameter passed through a given distance. As the measured values were scattered at every measurement, the surface drift velocity were obtained from the average of about ten measurements. Fig. 5 shows the results of the surface drift current at the two sections as a function of the reference air velocity U_r. As the results are indicated without distinction of the measurement conditions, they are very scattered. Nevertheless, the surface drift current is about 3 % of the reference air velocity U_r and in agreement with the results of many authors.[3),4),5)]

The hydrogen bubbles method was used to observe the qualitative features of complex flow patterns of the drift current. The average drift current fell rapidly away from the water surface, became zero at some depth in water, d, which continually fluctuated about some mean value, and caused a weakly uniform reverse flow at further depth. The measured value of d was about 7 cm regardless of wind speed.

3. Theoretical Consideration

3.1. Equations of Motion

If it is assumed that the motions of the air and water flow are two-dimensional, incompressible and invicid, the equations of motion which govern them can be written as

$$\frac{\partial u}{\partial t} + U\frac{\partial u}{\partial x} + wU' = -\frac{1}{\rho}\frac{\partial p}{\partial x}\ , \tag{1}$$

$$\frac{\partial w}{\partial t} + U\frac{\partial w}{\partial x} = -\frac{1}{\rho}\frac{\partial p}{\partial z}\ , \tag{2}$$

$$\frac{\partial u}{\partial x} + \frac{\partial w}{\partial z} = 0\ , \tag{3}$$

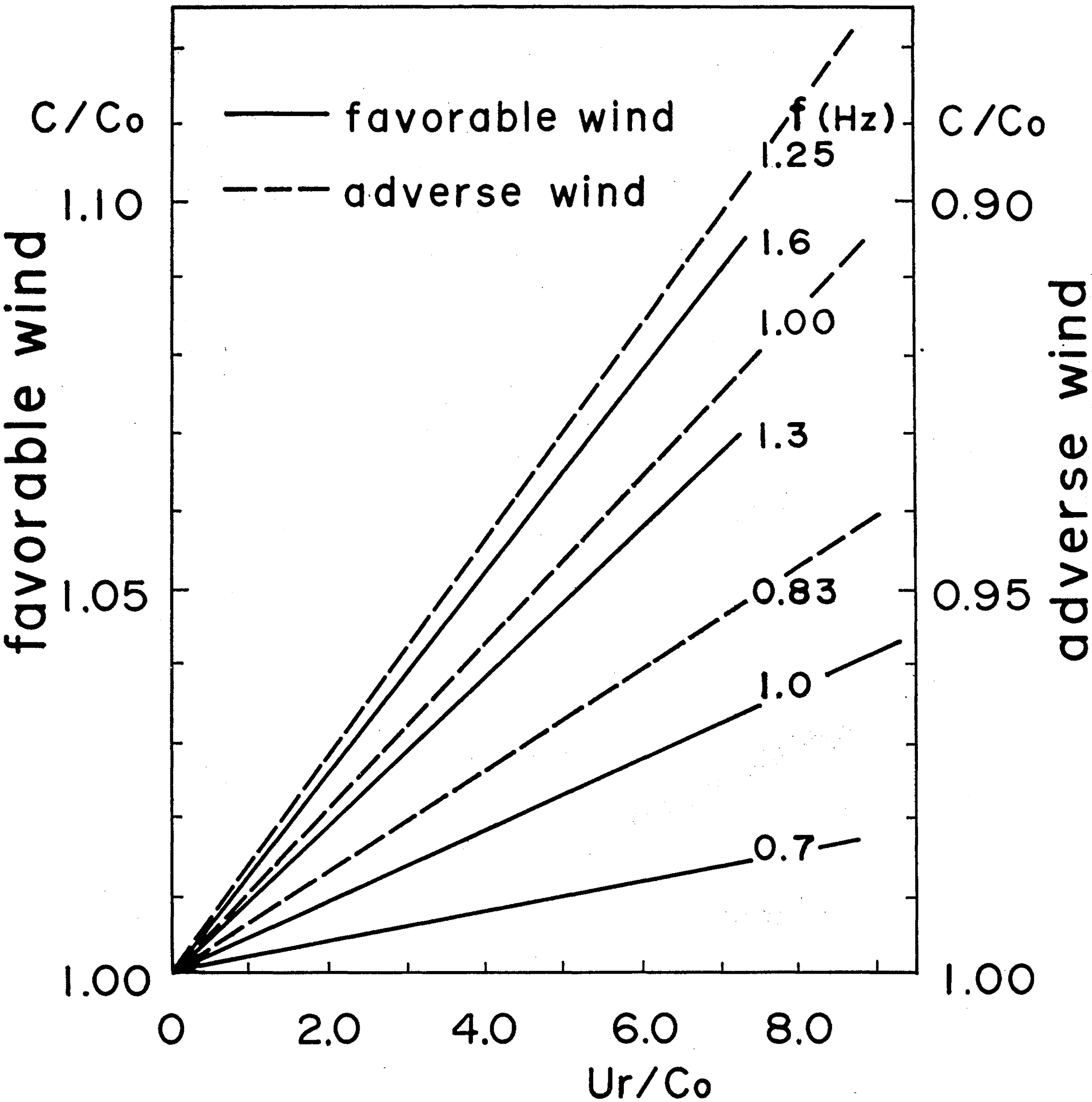

Fig. 4 Comparison of phase speed plotted against wind speed for the cases of a favorable wind (Shemdin) and of an adverse wind (present study).

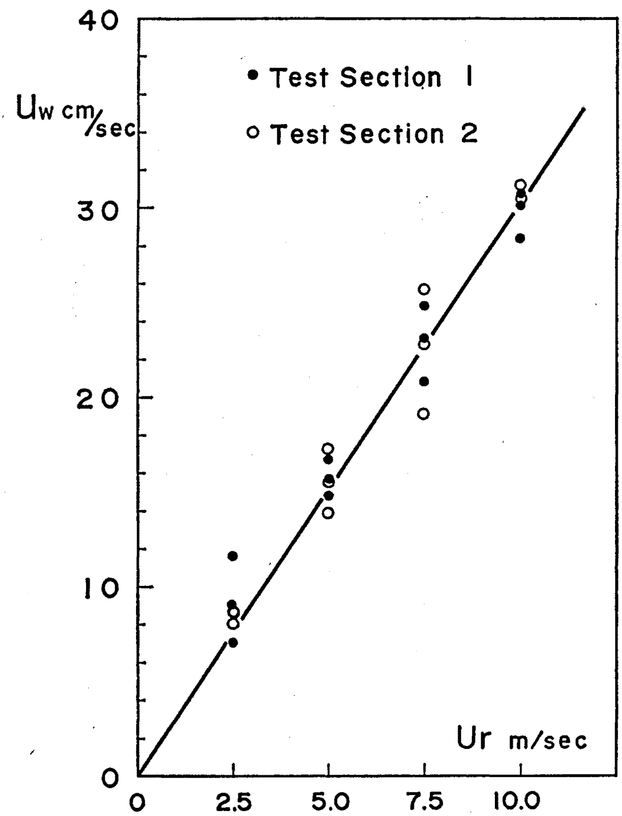

Fig. 5 Dependence of surface drift on wind speed, where test section 1 and 2 consist of a distance of 123cm near the station 4 and of 125cm near the station 2 respectively.

where the origin is taken on the undisturbed water surface, the co-ordinate (x, z) measured horizontally and vertically upwards respectively, (u, w) represent the wave-induced velocity components in these directions, U the horizontal component of the mean velocity which depends only on the vertical co-ordinate z, the prime the differentiation with respect to z, and p and ρ the wave-induced pressure and density of the fluid respectively. Let a stream function denote by ψ, then the perturbed velocity components (u, w) are given by

$$u = -\frac{\partial \psi}{\partial z}\,, \quad w = \frac{\partial \psi}{\partial x}\,, \tag{4}$$

which satisfy the continuity equation (3). If the elevation of the free water surface, η, is given in the following sinusoidal form

$$\eta(x,t) = ae^{ik(x-ct)}\,, \tag{5}$$

then ψ and p will be represented respectively by

$$\psi = \phi(z)\eta(x, t) \ , \quad p = \tilde{p}(z)\eta(x, t) \ , \tag{6}$$

where a denotes the amplitude, k the wave number, and c the phase velocity. On substitution of (6) into (1) and (2), we obtain

$$\rho[(U-C)\phi' - U'\phi] = \tilde{p} \ , \tag{7}$$

$$\rho k^2(U-C)\phi = \tilde{p}' \ . \tag{8}$$

Eliminating $\tilde{p}$ from two equations (7) and (8), we obtain

$$(U-C)(\phi'' - k^2\phi) - U''\phi = 0 \ . \tag{9}$$

This is the well known invicid form of the Orr-Sommerfeld equation. If we add the hydrostatic term to equation (7), the pressure is given in the following form

$$P = \rho[(U-C)\phi' - U'\phi]\eta - \rho gz \ . \tag{10}$$

The dynamical and kinematical boundary conditions at the water surface $z = \eta(x, t)$ are given by

$$P_w = P_a \qquad at\ z = \eta \ , \tag{11}$$

and by

$$w_{z=\eta} = \frac{\partial \eta}{\partial t} + U\frac{\partial \eta}{\partial x} \qquad at\ z = \eta \ , \tag{12}$$

where the subscripts w and a indicate water and air respectively. On substitution of (4), (5) and (6) into (12), we obtain

$$\phi = U - C \qquad at\ z = \eta \ . \tag{13}$$

For the wave-induced aerodynamic pressure P_a *at* the water surface we shall use Miles' expression

$$P_a = \rho_a(\alpha + i\beta)U_1^2 k\eta \ , \quad U_1 = U_*/\kappa \ , \tag{14}$$

where $\alpha + i\beta$ is a dimensionless pressure coefficient, U_* the friction velocity of the air, and $\kappa(=0.4)$ the von Karman constant. If we restrict the problem to the adverse wind condition, there is no critical layer where $U=C$. Therefore, the imaginary part of the aerodynamic pressure, β, is zero. Thus, if we substitute equation (10) for P_w and equation (14) for P_a, equation (11) gives

$$(U_w - C)\phi'_w - U'_w\phi_w = g + \alpha\frac{\rho_a}{\rho_w}U_1^2 k \qquad \text{at } z = \eta \ , \tag{15}$$

where the hydrostatic pressure term for the air is neglected because $\rho_a/\rho_w \ll 1$.

3.2. Solutions for the Water

In order to obtain the phase velocity of waves moving on a flowing fluid with arbitrary velocity distribution, Lilly used a perturbation method, and derived an analytical solution particularly for a laminar parabolic profile with zero net transport. From the visual observation mentioned earlier we found that the drift current was dominant only near the water surface, so that Lilly's profile may not be a fair approximation to our present case. For the similar reason, Kato adopted the following parabolic current profile as a better approximation to the experiments.

$$\left.\begin{aligned} U &= U_w(z+d)^2/d^2 \qquad && (0 \geqq z \geqq -\mathrm{d}) \ , \\ U &= 0 && (-d \geqq z \geqq -h) \ , \end{aligned}\right\} \tag{16}$$

where U_w is the surface drift velocity of the water and d is the distance below the water surface over which the drift current extends, and both of them are determined experimentally. we shall also assume that the drift current profile is expressed in the form of equation (16) after Kato.

Now after Lilly we attempt series expansions in the form

$$\phi = \phi_0 + \varepsilon\phi_1 + \ldots\ldots \ , \tag{17}$$

$$C = C_0 + \varepsilon C_1 + \ldots\ldots \ , \tag{18}$$

and further

$$k = k_0 + \varepsilon k_1 + \ldots\ldots \ , \tag{19}$$

where ε $(=U_w/C_0)$ is a small parameter. It should be noted that in the present study k is also expanded in the power series of ε, though both Lilly and Kato regarded k as a conservative quantity. Since the period of the wave generator does not change during the measurements, it appears to be reasonable to consider that the wave period T rather than k is conserved for mechanically generated waves.

On substitution of (17), (18) and (19) into (9) and equating terms of the same power of ε (U_w is of the order of ε) we obtain

$$\left.\begin{aligned} \phi_0'' - k_0^2\phi_0 &= 0 \ , \\ \phi_0'' - k_0^2\phi_1 &= -(U_w''/U_w + 2C_1/C_0k_0^2)\phi_0 . \end{aligned}\right\} \tag{20}$$

The boundary conditions (13) and (15) at the water surface $z=0$ similarly lead to the following equations

$$\phi_0 = -C_0 \ , \quad \phi_1 = C_0 - C_1 \ , \tag{21}$$

$$\phi_0' = -\frac{g}{C_0} \ , \quad \phi_1' = \left(1 - \frac{C_1}{C_0}\right)\phi_0' - \frac{U_w}{U_w}\phi_0 - \frac{\alpha g}{U_w}\frac{\rho_a}{\rho_w}\left(\frac{U_1}{C_0}\right)^2 \tanh k_0 h \ . \tag{22}$$

and the boundary condition at the base $z=-h$, $\phi=0$, gives

$$\phi_0 = \phi_1 = \ldots = 0 \ , \tag{23}$$

where $\frac{\rho_a}{\rho_w}\left(\frac{U_1}{C_0}\right)^2$, which is included in the last term of equation (22), is assumed to be of the same order of magnitude as ε. From the zeroth order solution of (20) to (23), we obtain for the stream function and wave speed

$$\phi_0 = -C_0\frac{\sinh k_0(z+h)}{\sinh k_0h} \ , \quad C_0^2 = g/k_0 \tanh k_0h \ . \tag{24}$$

Since the calculations of the first order solution for the assumed parabolic current profile (16) are very much tedious (see Kato for further details of the calculations), we present here only the following final results of the calculations

$$\frac{C}{C_0} = 1 + \frac{1}{K}\left[\varepsilon\frac{\overline{C}_1}{C_0} + \frac{1}{2}\alpha\frac{\rho_a}{\rho_w}\left(\frac{U_1}{C_0}\right)^2 \tanh k_0h\right] , \tag{25}$$

where

$$K = \frac{1}{2}\left[1 + \cosh 2k_0d - \coth 2k_0h \cdot \sinh 2k_0d + \frac{2k_0d}{\sinh 2k_0h}\right] , \tag{26}$$

$$\frac{\overline{C}_1}{C_0} = \frac{1}{k_0^2d^2}\left[\coth 2k_0h(\sinh k_0d \cdot \cosh k_0d - k_0d) - \sinh^2 k_0d + k_0^2d^2\right] , \tag{27}$$

and C_1 is equal to $\overline{C}_1/K$. For deep water these equations are simplified as follows:

$$K = \frac{1}{2}(1 + e^{-2k_0d}) \ , \tag{28}$$

$$\frac{\overline{C}_1}{C_0} = \frac{1}{2k_0^2d^2}\left[1 - e^{-2k_0d} + 2(k_0^2d^2 - k_0d)\right] , \tag{29}$$

and furthermore, for the limiting case of high wave number ($k_0d \gg 1$),

$$K \to \frac{1}{2} \ , \quad \frac{\overline{C}_1}{C_0} \to 1 \ . \tag{30}$$

Thus, the phase speed correction, C_1/C_0, which is the first correction term of equation (25), approaches two times the surface current.

On the other hand, if wave number k is conserved instead of T, then the boundary conditions (21) and (22) remain unaltered but in the equations of motion the last term, $2c/c_0k_0$, must be excluded from the right hand side of the first order equation of (20). As a results of the caluculations, since K becomes equal to 1, $C_1/C_0=\overline{C}_1/C_0$. Thus, $\overline{C}_1/C_0$ of equation (27) corresponds to the first order solution of the wave speed correction for the case that wave number k is conserved.

3.3. Solutions for the Air

We shall now obtain a numerical solution for the invicid Orr-Sommerfeld equation (9), to determine the non-dimensional pressure coefficient α for the case that the wind blows in the direction opposite to mechanically generated waves. The mean air velocity profile is assumed to be described by a logarithmic distribution and a uniform free stream distribution part, which appears to be a fair approximation to the experimental results,

$$\left.\begin{aligned} &U = U_r (=\text{constant}) && (H \geqq z \geqq z_r)\ , \\ &U = U_1 \log\frac{z}{z_0}\ , \quad U_1 = U_*/\kappa && (z_r \geqq z \geqq z_0)\ , \end{aligned}\right\} \tag{31}$$

$$\text{where } z_r = z_0 \exp\frac{Ur}{U_1}\ .$$

The boundary conditions are given at the roof by

$$\phi = 0 \qquad \text{at } z = H\ , \tag{32}$$

which means that there is no vertical motion at the rigid surface, and at the water surface by

$$\phi = C_0 \qquad \text{at } z = z_0\ , \tag{33}$$

by the requirement that the water surface remain a streamline (Miles[6] 1957) and that $U=0$ at $z=z_0$ from (31).

The numerical solution of the invicid Orr-Sommerfeld equation for the case of a favorable wind with the logarithmic velocity profile was first obtained by Conte & Miles (1959).[7] However, their procedure was very much complex because the equation involves a regular singularity at the critical layer where $U=c$. On the other hand, in the case of an adverse wind, since there is no critical layer the equation (9) has no singular point, and we shall be able to obtain the numerical solution with a simple standard procedure, as indicated below.

In the first place we attempt to obtain the solutions of equation (9) under the following initial conditions

$$\bar{\phi} = 0 \text{ and } \bar{\phi}' = -k_0 \qquad \text{at } z = H\ , \tag{34}$$

where $\bar{\phi}$ is used in place of ϕ. Since U is constant in the interval $H \geqq z \geqq z_r$ the stream function $\bar{\phi}$ is solved analytically in this range as

$$\bar{\phi} = -\sinh k_0(z-H) \qquad (H \geqq z \geqq z_r). \tag{35}$$

In the interval $z_r \geqq z \geqq z_0$, by starting from the initial conditions $\bar{\phi}(z_r)$ and $\bar{\phi}'(z_r)$ at $z=z_r$, equation (9) is numerically integrated in the negative direction from z_r to z_o by the Runge-Kutta-Gill method. The solutions $\bar{\phi}$ which are obtained in the way described sbove will not necessarily satisfy the boundary condition

(33) at $z=z_0$. Therefore, in order to derive the solutions which satisfy the boundary condition (33) from $\bar{\phi}(z)$, we put

$$\phi(z)=\frac{C_0}{\bar{\phi}(z_0)}\bar{\phi}(z) \text{ and } \phi'(z)=\frac{C_0}{\bar{\phi}(z_0)}\bar{\phi}'(z) . \tag{36}$$

It is obvious that ϕ and ϕ' give the solutions of equation (9) which satisfy the two boundary conditions (32) and (33).

Now the wave-induced pressure can be obtained from either equation (7) or (8) as follows:

$$\tilde{p}(z) = \rho_a[(U+C_0)\phi'(z)-U'(z)\phi(z)] , \tag{37}$$

or

$$\tilde{p}(z) = \rho_a[(U_r+C_0)\phi'(H) - k_0^2\int_z^H (U+C_0)\phi(z)dz] , \tag{38}$$

and α from the pressure $\tilde{p}$ at $z=z_0$ by

$$\alpha=\frac{1}{\rho_a U_1^2 k_0}\tilde{p}(z_0) . \tag{39}$$

4. Comparison with the Experimental Results

Before going into the comparison with the experimental results, we describe some qualitative features of the theoretical solutions (25). For that purpose we rewrite equation (25) in the following form which is convenient for comparison with the experiments

$$\frac{C}{C_0}=1+\frac{C_w}{C_0}+\frac{C_a}{C_0} , \tag{40}$$

where

$$\frac{C_w}{C_0}=\frac{U_w\bar{C}_1}{K\,C_0^2} , \quad \frac{C_a}{C_0}=\frac{\alpha}{2K}\frac{\rho_a}{\rho_w}\left(\frac{U_1}{C_0}\right)^2\tanh k_0h . \tag{41}$$

Of the two terms which influence wave speed, the first term, c_w/c_0, is proportional to surface current and thus to wind speed, and is positive or negative according to a favorable or adverse wind. If only the first term is regarded as dominant it will be impossible to explain the experimental facts that the dependence of the wave speed on wind speed is very different between a favorable and adverse wind condition. On the other hand, the aerodynamic term, c_a/c_0, is always negative because it is proportional to wind speed squared and the parameter α is a negative one. It follows that if both terms make an effective contribution to wave speed, the wave speed will decrease more significantly in an adverse wind codition than it will increase in a favorable wind condition. This conclusion qualitatively agrees with the experimental results of Fig. 4. Let us now calculate each term of equation (40). From the experimental conditions $H=45$ cm, $h=35$ cm, $d=7$ cm and $\rho_a/\rho_w=1.3\times10^{-3}$. For values of U_* and z_0 the experimental values at the station 4 were used. The calculated results are summarized in Table 3 for waves of different periods. The parameters α_1 and α_2 in the fifth and sixth columns of Table 3 are those values of α which have been calculated from equation (37) and (38), respectively. They are only slightly different because the mean velocity gradient is discontinuous at the junction point z_r of the air velocity profile (31). The parameter α_1 was used for the calculation of phase speed. $-c_w/c_0$ in the seventh column was calculated by using the relation $\varepsilon = 0.03 \times U_r/C_0$

Now it is of interest to compare the order of magnitude of $-c_w/c_0$ with that of $-c_a/c_0$. As an example, both of them are plotted against wave frequency, f, in Fig. 6 for the particular case that the reference air velocity U_r is 10 m/sec. It can be seen that $-c_w/c_0$ is 0.2 at most and tends to increase gradually with wave frequency. On the other hand, $-c_a/c_0$ varies very rapidly with wave frequency. Thus it is obvious from Fig. 6 that the aerodynamic term $-c_a/c_0$,

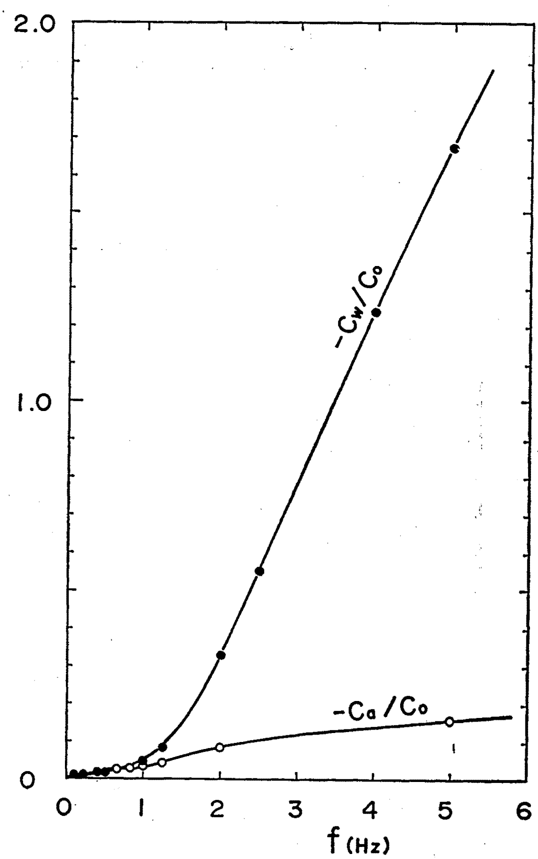

Fig. 6 Comparison of the phase-speed correction term due to drift current C_w/C_o, with that due to wave-induced aerodynamic pressure C_a/C_o, for the case of U_r=10m/sec, H=45 cm, h=35 cm, d=7 cm.

can not be neglected in the present experimental conditions because the wave frequency is in the range of $f=0.83\sim1.25$ Hz.

The values c/c_0 in the last column are compared with the experimental results in Fig. 7, where the theoretical results are represented by solid lines which connect the calculated values of c/c_0, and the experimental values by circular symbols. Both agree quite well for the wave data of $T=0.8$ and 1.0 sec within the range of the experimental errors, but for the wave of $T=1.2$ sec the calculated results give a little higher estimation than the experimental values. Some discrepancy between the theory and the experiment for the set of wave data of $T=1.2$ sec may be attributed partly to the rough approximation of the assumed current profile (16). Indeed, recent detailed laboratory study on the measurements of drift profile made by Dobroklonskiy and Lesnikov[8] shows that the current profile varies logarithmcally with depth in the upper layer of water.

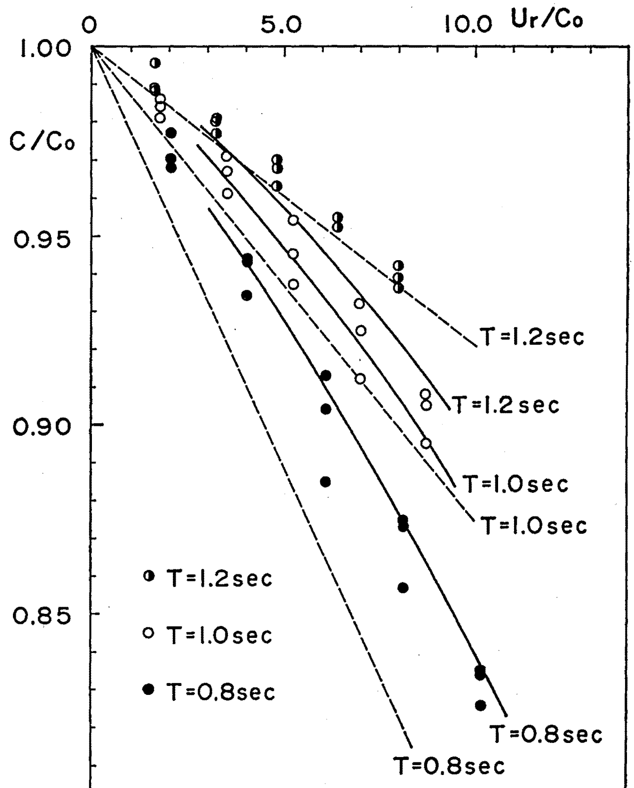

Fig. 7 Dependence of phase speed on wind speed from theoretical and experimental results. Solid lines indicate the present theoretical results and broken lines Lilly's solutions for laminar parabolic current profile with return flow.

Furthermore, let us compare the experimental values with the Lilly's solution of wave speed for the case of a laminar parabolic current profile with return flow. Lilly's solutions are indicated in Fig. 7 by the broken lines. We remark that since wave period is conserved in the present experiments, Lilly's expressin for the first order phase speed corrections is modified into

$$\frac{C_1}{C_0}=2\left[1-\frac{1+2\cosh(2k_0h)}{k_0h\sinh(2k_0h)}+\frac{3}{2k_0^2h^2}\right]\Big/\left(1+\frac{2k_0h}{\sinh 2k_0h}\right) . \tag{42}$$

Lilly's solutions consider only the drift current, so that it is certain that if the aerodynamic term is added to them, the resulting solutions would depart more significantly from the experimental vaules. Thus a better agreement with the experimental results is unlikely to be obtained from Lilly's solutions for the laminar parabolic profile.

5. Conclusion

Lavoratory study was made in the wind-wave tunnel on the effect of an adverse wind on the phase speed of mechanically generated waves, and the results were compared with those of theoretical analysis.

1) The phase speed of waves decreased remarkably with wind speed, and the rate of decrease increased with decreasing wave period.

2) The comparison of Shemdin's experimental results on wave speed with ours rather clearly shows that for waves of the same period the wave speed decreases in the adverse wind more significantly than it increases in the favorable wind.

3) It is suggested that the above experimental fact can be explained qualitatively by considering both the effects of the drift current and of the wave-induced aerodynamic pressure.

4) The results of the theoretical analysis were compared with the experimental results for three sets of wave data. Both agreed very well for two sets of wave data, but a little discrepancy was found for the remaining one.

Acknowldgements

The authors wish to express their thanks to Dr. Takematsu for his valuable advice. They are also indebted to the co-oparation of both Mr. Eto and Mr. Tanaka in carring out the experiment, and to Miss Noguchi for the typing of the manuscript. A part of this research was supported by scientific research fund of the Ministry of Education.

Table 1 Characteristics of air flow above water at various wind velocities. (a) case of wind waves alone, (b) case of coexsistence system of wind waves and mechanically generated waves.

Table 1 (a)

U_r (m/sec)	Station 2		Station 4		Station 6	
	U^* (cm/sec)	Z_0(cm)$\times10^3$	U_* (cm/sec)	Z_0(cm)$\times10^3$	U_* (cm/sec)	Z_0(cm)$\times10^3$
5.0	0.237	4.21	0.213	1.67	0.185	1.37
7.5	0.430	21.3	0.374	8.36	0.320	6.24
10.0	0.590	22.9	0.484	8.85	0.380	2.80
12.5	0.910	71.4	0.672	16.6	0.473	2.99
15.0	1.45	254	1.13	105	0.621	5.43

Table 1 (b)

U_r(m/sec)	Station 2		Station 4		Station 6	
	U_* (cm/sec)	Z_0(cm)$\times10^3$	U_* (cm/sec)	Z_0(cm)$\times10^3$	U_*(cm/sec)	Z_0(cm)$\times10^3$
5.0	0.237	4.59	0.236	4.20	0.220	4,54
7.5	0.457	27.8	0.418	18.7	0.378	17.0
10.0	0.594	25.3	0.587	26.1	0.539	25.7
12.5	0.926	80.3	0.676	18.1	0.598	13.0
15.0	1.47	277	1.10	91.3	0.636	7.06

Table 2 Experimental values of phase speed for various wind speeds. (a) wave period T=0.8sec, (b) T=1.0sec, (c)T=1.2sec. H_o: amplitude of incident waves (by estimate), L: wave length.

Table 2 (a)

H_0 (cm)	U_r(m/sec)	T (sec)	L (cm)	C (cm/sec)	C_0(cm/sec)	C/C_0	U_r/C_0
1.5	0.0	0.796	97.2	122.1	121.6	1.005	0.0
	2.5	0.801	94.9	118.5	122.2	0.970	2.05
	5.0	0.806	93.3	115.8	122.8	0.943	4.07
	7.5	0.806	90.4	112.2	122.8	0.913	6.11
	10.0	0.809	87.2	107.8	123.2	0.875	8.12
	12.5	0.807	82.7	102.5	122.9	0.834	10.17
2.5	0.0	0.798	97.0	121.6	121.8	0.998	0.0
	2.5	0.799	94.3	118.0	121.9	0.968	2.05
	5.0	0.803	91.8	114.3	122.4	0.934	4.08
	7.5	0.805	89.3	110.9	122.7	0.904	6.11
	10.0	0.804	86.0	117.0	122.6	0.873	8.16
	12.5	0.806	82.6	102.5	122.8	0.835	10.18
4.0	0.0	0.802	98.2	122.4	122.3	1.001	0.0
	2.5	0.803	96.0	119.6	122.4	0.977	2.04
	5.0	0.806	93.3	115.8	122.8	0.943	4.07
	7.5	0.808	88.0	108.9	123.0	0.885	6.10
	10.0	0.804	84.4	105.0	122.6	0.857	8.16
	12.5	0.804	81.4	101.2	122.6	0.826	10.20

Table 2 (b)

H_0 (cm)	U_r (m/sec)	T (sec)	L (cm)	C (cm/sec)	C_0 (cm/sec	C/C_0	U_r/C_0
1.5	0.0	1.006	143.1	142.3	142.9	0.996	0.0
	2.5	1.004	140.5	139.9	142.7	0.981	1.75
	5.0	1.006	139.5	138.7	142.9	0.971	3.50
	7.5	1.010	138.0	136.6	143.2	0.954	5.25
	10.0	1.014	135.6	133.7	143.5	0.932	6.97
	12.5	1.012	131.7	130.1	143.3	0.908	8.72
2.5	0.0	0.996	141.3	141.9	142.1	0,999	0.0
	2.5	0.994	139.0	139.8	141.9	0.986	1.76
	5.0	0.999	137.5	137.6	142.3	0.967	3.51
	7.5	1.001	134.8	134.7	142.5	0.945	5.26
	10.0	1.002	132.1	131.8	142.5	0.925	7.02
	12.5	1.003	129.4	129.0	142.6	0.905	8.76
4.0	0.0	0.999	142.5	142.6	142.3	1.002	0.0
	2.5	0.998	139.6	139.9	142.2	0.984	1.76
	5.0	1.001	137.1	137.0	142.5	0.961	3.51
	7.5	1.000	133.4	133.4	142.4	0.937	5.27
	10.0	1.001	130.1	130.0	142.5	0.912	7.02
	12.5	1.004	128.2	127.7	142.7	0.895	8.76

Table 2 (c)

H_0 (cm)	U_r (m/sec)	T (sec)	L (cm)	C (cm/sec)	C_0(cm/sec)	C/C_0	U_r/C_0
1.5	0.0	1.200	185.2	154.3	155.0	0.996	0.0
	2.5	1.203	184.5	153.4	155.2	0.989	1.61
	5.0	1.210	184.5	152.5	155.5	0.981	3.22
	7.5	1.217	184.0	151.2	155.8	0.970	4.81
	10.0	1.220	181.8	149.0	156.0	0.955	6.41
	12.5	1.225	179.6	146.6	156.2	0.939	8.00
2.5	0.0	1.201	186.1	155.0	155.1	0.999	0.0
	2.5	1.203	184.4	153.3	155.2	0.988	1.61
	5.0	1.206	183.0	151.7	155.3	0.977	3.22
	7.5	1.213	181.8	149.9	155.6	0.963	4.82
	10.0	1.213	179.7	148.2	155.6	0.952	6.43
	12.5	1.213	176.7	145.7	155.6	0.936	8.03
4.0	0.0	1.119	186.4	155.5	155.0	1.003	0.0
	2.5	1.203	185.9	154.5	155.2	0.996	1.61
	5.0	1.214	185.3	152.6	155.7	0.980	3.21
	7.5	1.219	184.0	150.9	155.9	0.968	4.81
	10.0	1.223	182.3	149.1	156.1	0.955	6.41
	12.5	1.225	180.2	147.1	156.2	0.942	8.00

Table 3 Results of theoretical calculation of phase speed for mechanically generated waves of various periods. Water depth h=35 cm, height from water surface to ceiling H=45cm, thickness of uppermost, strongly mixed water layer d=7cm.

T(sec)	U_r (m/sec)	C_0 (m/sec)	U_r/C_0	$-\alpha_1$	$-\alpha_2$	$-C_w/C_0$ $\times 10^2$	$-C_A/C_0$ $\times 10^2$	C/C_0
0. 5	5. 0	0. 780	6. 41	67. 7	66. 9	16. 2	3. 71	0. 801
	7. 5		9. 62	34. 0	33. 7	24. 3	5. 74	0. 700
	10. 0		12. 82	30. 5	30. 3	32. 4	8. 64	0. 590
	12. 5		16. 03	21. 1	21. 0	40. 5	11. 5	0. 480
0. 8	5. 0	1. 221	4. 10	95. 0	98. 6	4. 19	1. 61	0. 942
	7. 5		6. 14	54. 0	53. 0	6. 28	2. 82	0. 909
	10. 0		8. 19	48. 4	47. 9	8. 38	4. 23	0. 874
	12. 5		10. 24	35. 4	34. 9	10. 5	5. 98	0. 835
1. 0	5. 0	1. 425	3. 51	108	116	2. 36	1. 12	0. 965
	7. 5		5. 26	65. 4	63. 4	3. 54	2. 10	0. 944
	10. 0		7. 02	58. 3	57. 5	4. 72	3. 14	0. 921
	12. 5		8. 77	43. 4	42. 2	5. 90	4. 49	0. 896
1. 2	5. 0	1. 511	3. 22	119	133	1. 63	0. 89	0. 975
	7. 5		4. 84	76. 2	73. 1	2. 44	1. 75	0. 958
	10. 0		6. 45	67. 8	66. 6	3. 26	2. 61	0. 941
	12. 5		8. 06	50. 8	49. 0	4. 07	3. 76	0. 922
1. 5	5. 0	1. 658	3. 02	137	158	1. 16	0. 72	0. 981
	7. 5		4. 52	92. 3	87. 7	1. 73	1. 50	0. 968
	10. 0		6. 03	82. 0	80. 2	2. 31	2. 23	0. 955
	12. 5		7. 54	61. 8	59. 0	2. 89	3,23	0. 939

References

1) Lilly, D. K., On the speed of surface gravity waves propagating on a moving fluid, Appendix of a paper of Hidy and Plate, J. Fluid Mech., Vol. 26, 1966, pp. 683-686.
2) Kato, H., The calculation of wave speed for a parabolic current profile, from a paper of 19th conference on coastal engineering, 1972, pp. 113-118 (in Japanese).
3) Shemdin, O. H., Wind generated current and interaction with waves, from 13th international conference on coastal engineering, 1972, Vancouver, B. C., Canada.
4) Hidy, G. M. and Plate, E. J., Wind action on water standing in a laboratory channel, J. Fluid Mech., Vol. 26, 1966, pp. 651-688.
5) Bye, J. A. T., The wave-drift current, J. Mar. Res., Vol. 25, 1967, pp. 95-102.
6) Miles, J. W., On the generation of surface waves by shear flows, J. Fluid Mech., Vol. 3, 1957, pp. 185-204.
7) Conte, S. D. and Miles, J. W., on the numerical integration of the Orr-Sommerfeld equation, J. Soc. Indust. Appl. Math., Vol. 7, 1959, pp. 361-366.
8) Dobroklonskiy, S. V. and Lesnikov, B. M., Izv. Atmospheric and Oceanic Physics, Vol. 8, 1972, pp. 686-692.

(Received October 2, 1973)